

Synthesis of a Mineral–Organic Hybrid by Treatment of Phlogopite with Phenylphosphonic Acid

Camino Trobajo, Sergei A. Khainakov, Aránzazu Espina, and José R. García*

Departamento de Química Orgánica e Inorgánica, Universidad de Oviedo, 33006 Oviedo, Spain

Miguel A. Salvadó, Pilar Pertierra, and Santiago García-Granda

Departamento de Química-Física y Analítica, Universidad de Oviedo, 33006 Oviedo, Spain

Agustín Martín-Izard

Departamento de Geología, Universidad de Oviedo, 33015 Oviedo, Spain

Anatoly I. Bortun

ASEC Delphi Energy & Chassis Systems, 1301 Main Parkway, Catoosa, Oklahoma 74015

Received January 10, 2001. Revised Manuscript Received September 19, 2001

The reaction between natural phlogopite, having the idealized formula $\text{KMg}_3(\text{AlSi}_3\text{O}_{10})(\text{OH})_2$, and phenylphosphonic acid under soft conditions (24 h, 80 °C, reflux) originated a new layered material of the following idealized composition: $[\text{Mg}(\text{H}_2\text{O})_2]_{0.5}(\text{AlSi}_3\text{O}_6)(\text{O}_3\text{-PC}_6\text{H}_5)_2 \cdot 2\text{H}_2\text{O}$. The reaction mechanism involves the rupture of the trioctahedral layers of phlogopite and the formation of a new basal spacing of a hydrophobic type that is occupied by phenylphosphonic groups in a pseudomonomolecular arrangement. Simultaneously, the mobile K^+ ions become partially substituted by $[\text{Mg}(\text{H}_2\text{O})_2]^{2+}$ groups, a hydrophilic space of the vermiculite type thus being obtained.

Introduction

Layered inorganic compounds attract special attention due to their valuable and sometimes unique properties. The possibility and ease of tailored regulation of their structure via ion exchange or intercalation routes is another advantage that gives scientists extremely powerful tools for creating new compounds with desirable properties.

In 1978, Alberti et al.¹ demonstrated the possibility of synthesizing organic derivatives of metal(IV) phosphates and phosphonates possessing the general formula $\alpha\text{-Zr}(\text{O}_3\text{PR})_2 \cdot \text{Solv}$ or $\alpha\text{-Zr}(\text{O}_3\text{POR})_2 \cdot \text{Solv}$, where R is an organic group and Solv is an intercalated molecule (when present). It was found that these new hybrid compounds adopt the α -zirconium phosphate type structure,² which means a layered structure with tetrahedral $\text{O}_3\text{P-OH}$ groups replaced by tetrahedral $\text{O}_3\text{P-R}$ or $\text{O}_3\text{P-OR}$ moieties.³ Many organic derivatives with different functional groups (alkyl, aryl, alcoholic, amino, carboxylic, sulfonic, etc.) have been prepared since then.⁴ Moreover, single-phase mixed-derivative compounds with two types of R groups⁵ or different di-, tri-,

and tetravalent metals^{6,7} have been synthesized by using three different synthetic routes:

(i) from a mixed solution containing phosphoric and phosphonic acids in the presence of HF ,¹

(ii) by reaction in hydrothermal conditions,⁸ and

(iii) by partial or complete substitution of the interlayer HOPO_3^{2-} groups (in a preformed, layered phosphate) with the RPO_3^{2-} groups of a phosphonic acid.⁹

It is interesting that layered metal(IV) phosphates possess structural characteristics comparable to those of some phyllosilicates. Thirty years ago, α -zirconium phosphate was already being compared with montmorillonite,¹⁰ a typical representative of layered silicate minerals.¹¹ Bearing in mind their similarities, it would be interesting to attempt to extend the aforementioned

(5) Dines, M. B.; Di Giacomo, P.; Callahan, K. P.; Griffith, P. C.; Lane, R. H.; Cooksey, R. E. *ACS Symp. Ser.* **1982**, 192.

(6) (a) Dines, M. B.; Cooksey, R. E.; Griffith, P. C.; Lane, R. H. *Inorg. Chem.* **1983**, 22, 1003. (b) Cao, G.; Hong, H.-G.; Mallouk, T. E. *Acc. Chem. Res.* **1992**, 25, 420. (c) Thompson, M. E. *Chem. Mater.* **1994**, 6, 1168. (d) Alberti, G.; Casciola, M.; Costantino, U.; Vivani, R. *Adv. Mater.* **1996**, 8, 291. (e) Clearfield, A. *Solid State Mater. Sci.* **1996**, 1, 268.

(7) (a) Cao, G.; Mallouk, T. E. *Inorg. Chem.* **1991**, 30, 1434. (b) Scott, K. J.; Zhang, R.-C.; Clearfield, A. *Chem. Mater.* **1995**, 7, 1095. (c) Mason, M. R. *J. Cluster Sci.* **1998**, 9, 1.

(8) Jaimez, E.; Bortun, A. I.; Khainakov, S. A.; Voitko; I. I.; García, J. R.; Rodríguez, J. *J. Mater. Res.* **1998**, 13, 323.

(9) (a) Yamanaka, S.; Hattori, M. *Inorg. Chem.* **1981**, 20, 1929. (b) Yamanaka, S.; Sakamoto, K.; Hattori, M. *J. Phys. Chem.* **1984**, 88, 2067. (c) Alberti, G.; Murcia-Mascarós, S.; Vivani, R. *Mater. Chem. Phys.* **1993**, 35, 187.

(10) Leigh, D.; Dyer, A. *J. Inorg. Nucl. Chem.* **1972**, 34, 369.

(1) Alberti, G.; Costantino, U.; Allulli, S.; Tomassini, N. *J. Inorg. Nucl. Chem.* **1978**, 40, 1113.

(2) Troup, J. M.; Clearfield, A. *Inorg. Chem.* **1977**, 16, 3311.

(3) Poojary, D. M.; Bhardwaj, C.; Clearfield, A. *J. Mater. Chem.* **1995**, 5, 171.

(4) Alberti, A.; Costantino, U. In *Inclusion Compounds. Inorganic and Physical Aspects of Inclusion*; Atwood, J. L., Davies, J. E. D., MacNicol, D. D., Eds.; Oxford University Press: Oxford, 1991; Vol. 5.

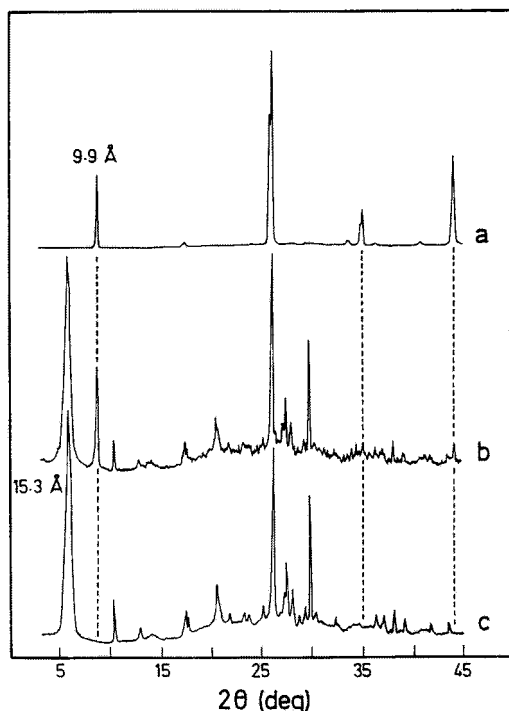


Figure 1. XRD powder patterns of phlogopite (a) and phlogopite treated with phenylphosphonic acid in (b) one step and (c) three steps.

approaches of creating organic–inorganic hybrid materials to natural minerals such as micas.

Mica is a generic name for a group of complex hydrous potassium–aluminum minerals that belong to the 2:1 layer silicates with tetrahedral (tet) sheets on either side of the octahedral (oct) sheet.¹² In the tet–oct–tet sandwich, the two opposing tetrahedral sheets are not directly opposite each other and there is an offset needed to produce octahedral coordination in the octahedral sheet.¹³ In micas, cation substitution in either the tetrahedral or octahedral sheets results in an overall negative charge in the layers which is compensated, and the layers are bonded together by large, positively charged interlayer cations, most commonly K^+ .¹⁴ The best known and most common found in nature of these are muscovite and phlogopite–biotite, which are, respectively, dioctahedral and trioctahedral micas. Phlogopite is quite abundant in nature. In this mica, Mg^{2+} occupies the trioctahedral sheet, Si^{4+} and Al^{3+} occupy tetrahedral sheets, and K^+ occupies the interlayer positions.

The aim of the current study was to examine the synthesis of organic–mineral derivative materials using route iii, namely, topotactic substitution of the mica's functional groups with organic radicals.

Experimental Section

Materials. The natural phlogopite sample came from a copper–gold magnesian skarn located in the Rio Narcea Gold

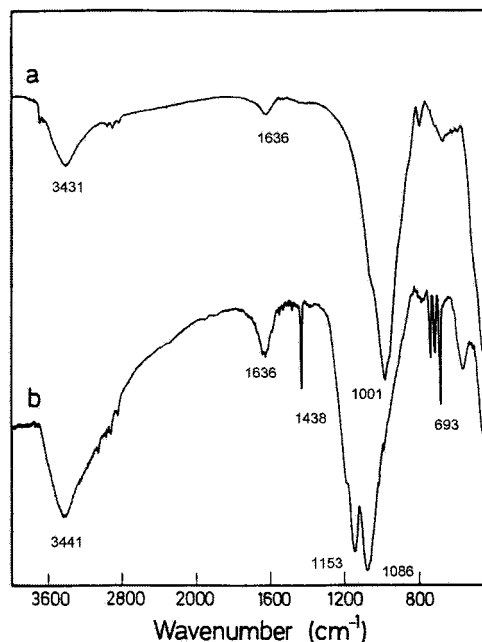


Figure 2. IR spectra of (a) phlogopite and (b) phlogopite treated with phenylphosphonic acid (three steps).

Belt, Central Asturias, Spain.¹⁵ Phlogopite is developed by a hydrothermal metasomatic reaction along the contact between a Cambrian dolostone and a Carboniferous monzogranite. Olivine and diopside were formed during a first metasomatic reaction. Subsequently, during a second hydrothermal stage, phlogopite was developed from diopside. In this case, phlogopite is the magnesium-rich member (average composition (wt %): Si, 17.9; Al, 7.3; Ti, 0.2; Mg, 13.8; Fe, 4.7; K, 8.9; Na, 0.1; F, 2.1).

Organic–mineral derivative compounds were prepared using the following procedure: 1 g sample of finely powdered phlogopite was treated with 50 mL of 1 M phenylphosphonic acid at 80 °C (water bath, constant shaking) for 24 h. The mica was then recovered by centrifugation and repeatedly treated with a new portion of 1 M phenylphosphonic acid five more times. After the final treatment, the phlogopite was washed with distilled water and dried at room temperature in air.

Both aluminum and magnesium chlorides were treated with phenylphosphonic acid following the same route described in the synthesis of the organic–mineral derivative compounds. Finely powdered $AlCl_3 \cdot 6H_2O$ (2.4 g) or $MgCl_2 \cdot 6H_2O$ (2.0 g) was treated with 50 mL of 1 M phenylphosphonic acid at 80 °C (water bath, constant shaking) for 24 h. The solids were recovered by centrifugation, washed with distilled water, and dried at room temperature in air.

Analytical Procedures. Microanalytical data (C and H) were obtained with a Perkin-Elmer 2400B elemental analyzer. Elemental analysis was performed on a Cameca SX-50 electron microprobe equipped with four wavelength-dispersive spectrometers with TAP, PET, and LIF analyzing crystals. Gas flow proportional counters using P-10 gas (90% argon, 10% methane) were used on all spectrometers. Analyses were conducted at a 15 kV accelerating voltage, a beam current of 15 nA, and a beam diameter of 3 μm (counting time 10 s). The powder diffractometer used was a Philips 1050 model (Cu $K\alpha$, 40 kV, and 30 mA). Thermal analysis was performed using a Mettler TA 4000 (TG 50, DSC 30, air atmosphere, and a heating rate of 10 °C min^{-1}). IR spectra were obtained on a Perkin-Elmer 1720-X FT spectrometer by the KBr pellet technique. ^{31}P MAS NMR spectra were obtained on a Bruker AC-300 spectrometer. SEM micrographs were recorded using a JEOL JSM-6100 electron microscope operating at 20 kV.

(11) (a) Grim, R. E. *Clay Mineralogy*, McGraw-Hill: New York, 1968. (b) Liebau, F. *Structural Chemistry of Silicates*, Springer-Verlag: Berlin, 1985.

(12) *Micas. Reviews in Mineralogy*, Bailey, S. W., Ed.; Mineralogical Society of America: Washington, DC, 1984; Vol. 13.

(13) Deer, W. A.; Howie, R. A.; Zussman, J. *An Introduction to the Rock Forming Minerals*, Longman: Hong Kong, 1992.

(14) Putnis, A. *Introduction to Mineral Sciences*, Cambridge University Press: Cambridge, 1992.

(15) Cepedal, A.; Martín-Izard, A.; Reguilón, R.; Rodríguez-Pevida, L.; Spiering, E.; González-Nistal, S. *J. Geochem. Explor.* **2000**, *71*, 119.

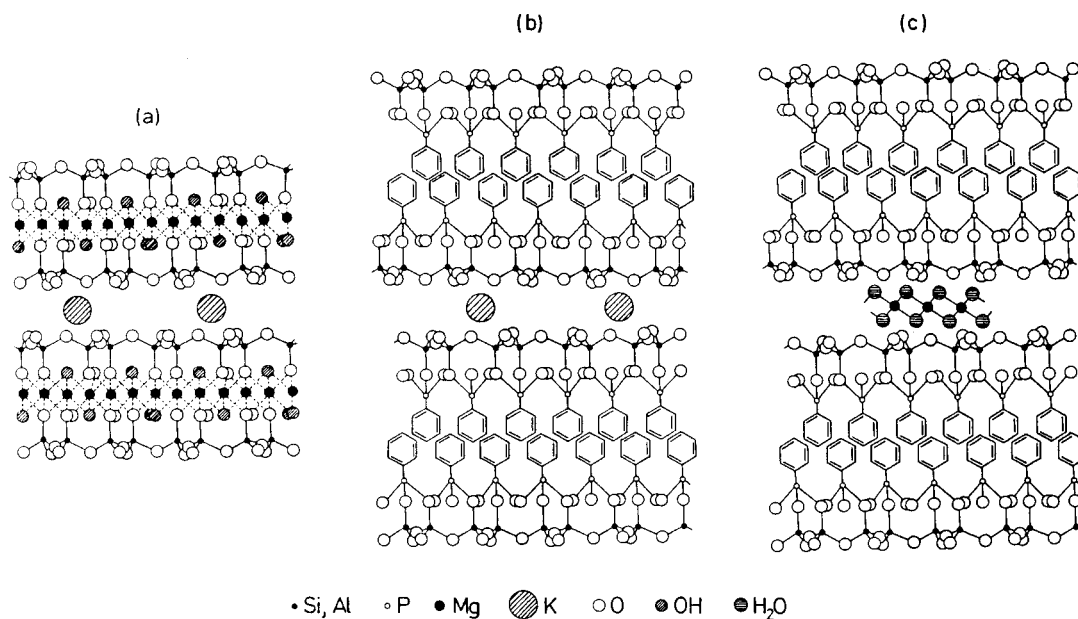


Figure 3. Idealized mechanism for the transformation of phlogopite into a mineral-organic hybrid material with vermiculite-type layers: (a) phlogopite, (b) destruction of the trioctahedral layer, anchorage of the phenylphosphonic groups, and formation of a hydrophobic area, (c) K^+ - $[Mg(H_2O)_2]^{2+}$ ion-exchange in the hydrophilic interlayer space and formation of a vermiculite-type hydrophilic area.

TEM micrographs were recorded using a JEOL 2000 EX-II electron microscope operating at 180 kV.

Structural Model. The structure plot and some of the modeling calculations were made using the PowderCell 2.1 program.¹⁶

Results and Discussion

Figure 1 shows the XRD powder patterns of phlogopite and the materials formed after its treatment with phenylphosphonic acid. It is seen that even a single treatment results in the formation of a new phase with a basal spacing of 15.3 Å, which coexists with an unmodified phlogopite phase ($d = 9.9$ Å). The 15.3 Å phase becomes the sole phase only after three successive treatments with phenylphosphonic acid.

A possible explanation of the experimental data could be that the strong acidity of the phenylphosphonic acid destroys the original structure, with the subsequent precipitation of insoluble metal phosphonates with an interlayer distance of 15.3 Å. However, additional facts indicate that this hypothesis should be discarded. Under our experimental conditions, the treatment of aluminum chloride with phenylphosphonic acid originates the formation of $Al(HO_3PC_6H_5)_3 \cdot H_2O$ with a interlayer distance of 14.5 Å ((experimental wt %) Al, 5.2; P, 17.9; C, 40.4; H, 3.5; weight loss at 800 °C, 47.2; (calculated wt %) Al, 5.23; P, 18.02; C, 41.86; H, 3.88; weight loss, 48.84).¹⁷ Similarly, when the starting solid of the process is magnesium chloride, the formation of $Mg(O_3PC_6H_5) \cdot H_2O$ with a basal spacing of 14.3 Å should be expected.¹⁸ However, under our experimental conditions, magnesium phenylphosphonate is not obtained. Thus, phlogopite derivative materials are not simple metal phosphonates.

The new materials were characterized using spectroscopic methods. The IR spectra shown in Figure 2 furnish some data that are helpful in the identification of the functional groups in the materials. Namely, the appearance of new bands at 693, 724, 748, and 1438 cm^{-1} , in addition to the characteristic bands for phlogopite, strongly suggests the presence of phenylphosphonic groups in the mica.¹⁹ This is in agreement with the ^{31}P MAS NMR data. The ^{31}P NMR spectrum present one wide peak, centered at -1.4 ppm, with their spinning sidebands. Considering that similar spectra were observed for metal(IV)-based phenylphosphonates,^{8,19} we may conclude that the phenylphosphonate groups have been incorporated into the phlogopite structure. Additionally, the broadness of the peak indicates a certain local disorder in the phosphorus environment.

According to the idealized formula, $KMg_3(AlSi_3O_{10})(OH)_2$, a schematic mechanism of the modification of the mica can be presented as in Figure 3. This process suggests the rupture of the trioctahedral layers of phlogopite, with the formation of a new basal spacing of a hydrophobic type occupied by phenylphosphonic groups. Simultaneously, the mobile K^+ ions would be partially substituted by $[Mg(H_2O)_2]^{2+}$ groups, a hydrophilic space of a vermiculite type thus being obtained. The idealized formula for the new mineral-organic hybrid compound might be represented as $[Mg(H_2O)_2]_{0.5}-(AlSi_3O_6)(O_3PC_6H_5)_2 \cdot nH_2O$. This material presents a segregation of hydrophobic groups from hydrophilic groups, previously described for Zr-based layered compounds.²⁰

(16) Kraus, W.; Nolze, G. *J. Appl. Crystallogr.* **1996**, *29*, 301.

(17) Cabeza, A.; Aranda, M. A. G.; Bruque, S.; Poojary, D. M.; Clearfield, A.; Sanz, J. *Inorg. Chem.* **1998**, *37*, 4168.

(18) Cao, G.; Lee, H.; Lynch, V. M.; Mallouk, T. E. *Inorg. Chem.* **1988**, *27*, 2781.

(19) Jaimez, E.; Bortun, A. I.; Hix, G. G.; García, J. R.; Rodríguez, J.; Slade, R. C. T. *J. Chem. Soc., Dalton Trans.* **1996**, 2285.

(20) Wang, J. D.; Clearfield, A.; Peng, G. Z. *Mater. Chem. Phys.* **1993**, *35*, 208.

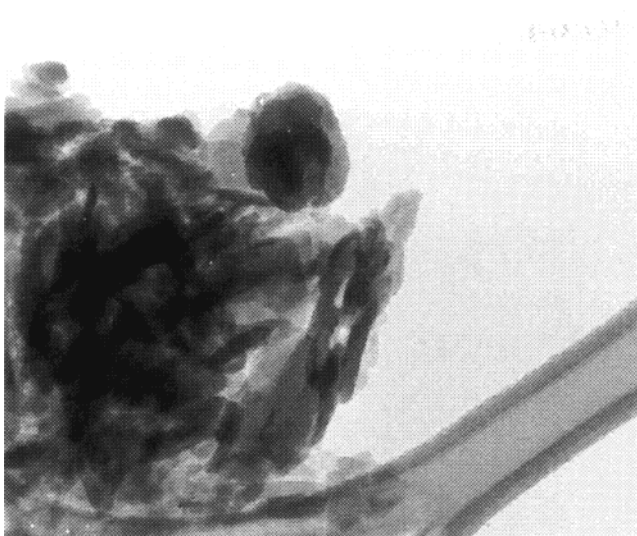
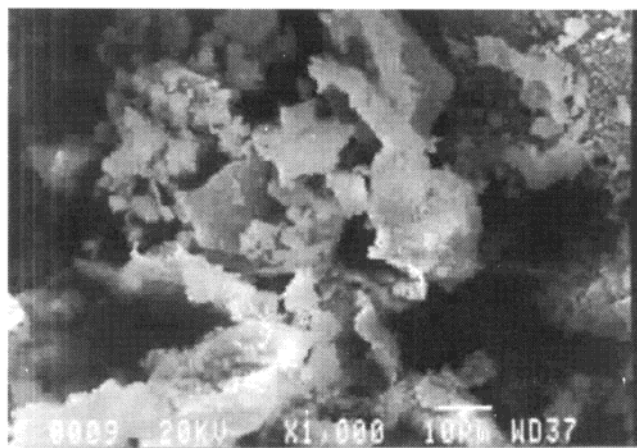


Figure 4. Electron microscopy images: (a, top) SEM image (1000 \times magnification, reproduced at 58% of original size) of the phlogopite treated with phenylphosphonic acid (one step) when the corrugated sheets (new material) of the phlogopite flakes can be distinguished, (b, bottom) TEM image (21000 \times magnification, reproduced at 71% of original size) of the mineral-organic hybrid material.

Table 1. Analytical Data and Experimental Weight Loss at 800 °C (in Air) of the New Mineral-Organic Hybrid Material and Those Calculated from the Formula $[\text{Mg}(\text{H}_2\text{O})_2]_{0.5}(\text{AlSi}_3\text{O}_6)(\text{O}_3\text{PC}_6\text{H}_5)_2 \cdot 2\text{H}_2\text{O}$

	exptl	calcd		exptl	calcd
% Si	13.2	14.36	% P	10.1	10.60
% Al	4.2	4.61	% C	23.4	24.62
% Mg	1.3	2.08	% H	2.5	2.39
% Fe	0.4		% weight loss	33.5	32.81
% K	0.9				

In nature, under meteoric conditions, phlogopite transforms to vermiculite.²¹ During vermiculitization, the loss of K^+ from the parent mica causes a charge imbalance, which may be compensated in different ways. Gruner²² was the first to suggest that the charge deficit is partly compensated by Fe^{2+} oxidation to Fe^{3+} , or by the introduction of H^+ . Several authors have investigated this process thoroughly, particularly in

(21) (a) Basset, W. A. *Am. Miner.* **1959**, *44*, 282. (b) *Hydrous Phyllosilicates. Reviews in Mineralogy*; Bailey, S. W., Ed.; Mineralogical Society of America: Washington, DC, 1988; Vol. 19.

(22) Gruner, J. W. *Am. Miner.* **1934**, *19*, 557.

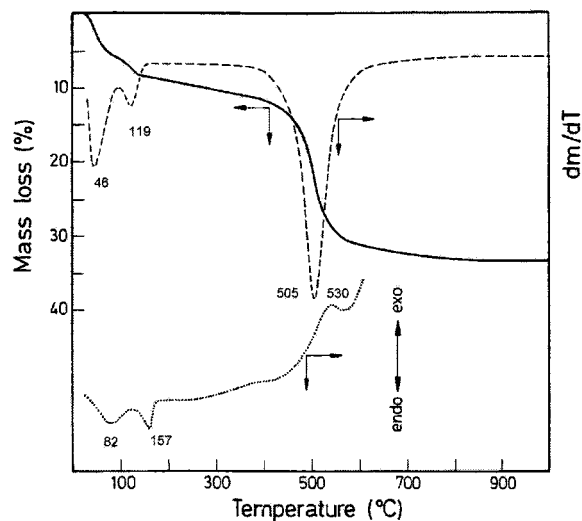


Figure 5. TG (—), DTG (---) and DSC (···) curves for the mineral-organic hybrid material.

soils, and have identified the different parameters that connect vermiculitization and oxidation. These parameters include the chemical composition of the parent mica and particularly its Fe^{2+} content,²³ the chemical properties of the geological environments, i.e., the redox conditions or the Fe^{3+} activity,²⁴ and the structural modifications, i.e., the loss of octahedral Fe ,²⁵ upon vermiculitization. A quite different vermiculitization process which is completely independent of the Fe content of the parental mica has been suggested by Barshad,²⁶ who proposed that the charge deficit is essentially balanced in the interlayer and that the replacement of K^+ by Mg^{2+} is accompanied by hydration. Summarizing, the octahedral sheet participates actively in the reaction, and its composition changes during the vermiculitization although, evidently, the most important changes are observed in the interlamellar space.

The morphology of the 15.3 Å phase is similar to that of the minerals of the vermiculite group. As occurs in nature, the SEM image (Figure 4a) shows that the new mineral-organic hybrid (lighter in color) replaces phlogopite flakes (darker in color). We can see how the corrugated sheets of the new material grow on the phlogopite flakes in which some crystal form (rectangular) and cleavage can be distinguished. In the new material the cleavage, more open than in phlogopite, very irregular, can also be seen. The layered structure preservation of the mineral-organic hybrid has been proven by transmission electron microscopy (Figure 4b).

Table 1 shows the analytical data and the mass losses after calcination at 800 °C in air for the new material in comparison with the theoretical ones derived from the formula $[\text{Mg}(\text{H}_2\text{O})_2]_{0.5}(\text{AlSi}_3\text{O}_6)(\text{O}_3\text{PC}_6\text{H}_5)_2 \cdot 2\text{H}_2\text{O}$. Considering that the starting material was a natural mineral, the agreement between experimental and theoretical data is excellent. The fact that the concentration of magnesium is significantly lower than the one

(23) Roy, R.; Romo, L. A. *J. Geol.* **1957**, *65*, 603.

(24) (a) Wilson, M. J. *Clay Miner.* **1970**, *8*, 291. (b) Bouda S.; Isaac, K. P. *Clay Miner.* **1986**, *21*, 149. (c) Graf v. Reichenbach, H.; Beyme, B. *Clay Miner.* **1988**, *23*, 261.

(25) Farmer, V. C.; Russell, J. D.; McHardy, W. J.; Newman, A. C. D.; Ahlrichs, J. L.; Rimsaite, J. Y. H. *Miner. Magn.* **1971**, *38*, 121.

(26) Barshad, I. *Am. Miner.* **1948**, *33*, 655.

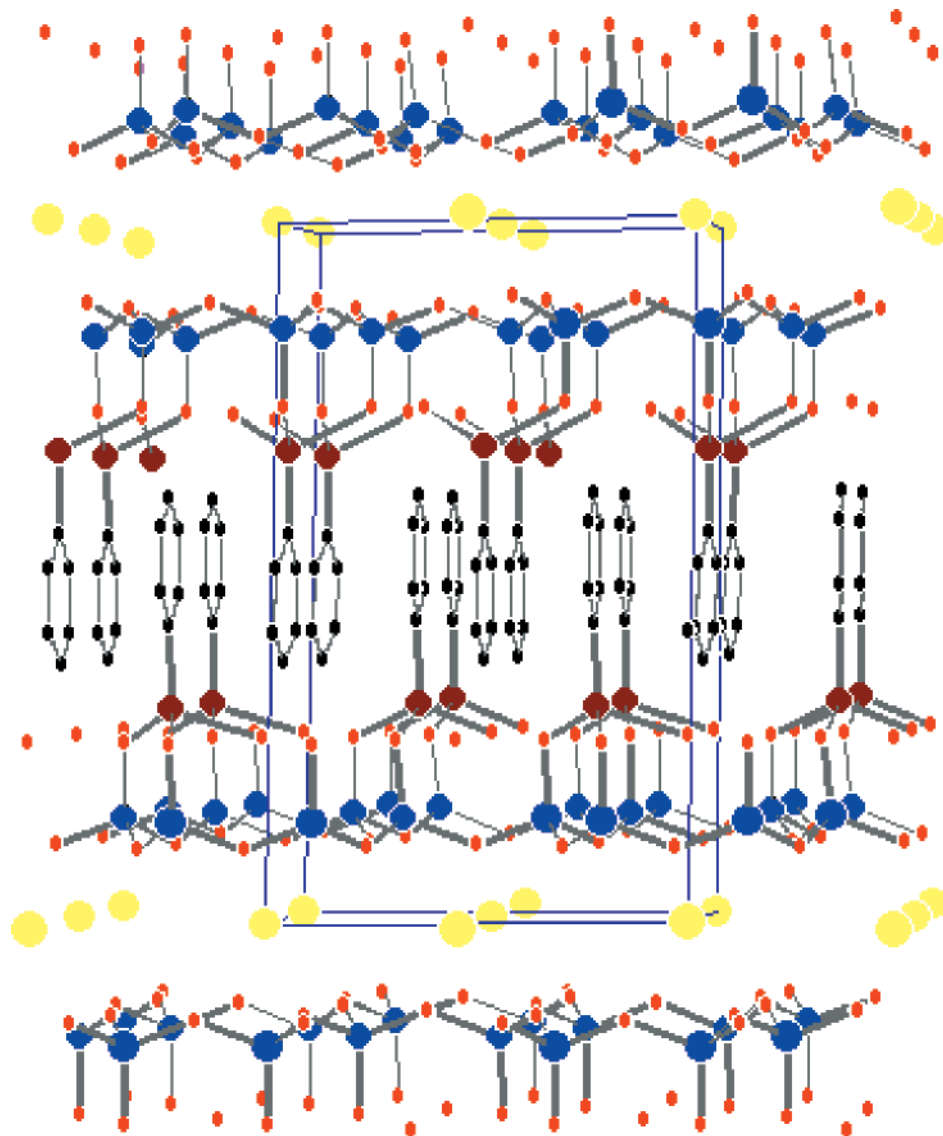


Figure 6. Proposed structure for the $\text{K}(\text{AlSi}_3\text{O}_6)(\text{O}_3\text{PC}_6\text{H}_5)_2$ intermediate compound viewed along the a -axis (black, carbon; blue, silicon; red, oxygen; brown, phosphorus; yellow, potassium; hydrogen atoms not shown for greater clarity).

calculated and that the concentration of both iron and potassium is appreciable indicates that K^+ and perhaps Fe^{2+} compensate for the Mg^{2+} shortage.

Analysis of TG data (Figure 5) shows that the thermal decomposition of the new material occurs in three steps. In the first stage, which takes place in the temperature range 50–130 °C, the hydration water is released. The weight loss in the second stage (130–180 °C) is connected to the release of water coordinated to the magnesium ion, and the basal spacing decreasing to 15.0 Å. The oxidation of the organic phenylphosphonic group takes place at a higher temperature. Accordingly, the DSC curve also has three peaks. Two endothermic peaks are clearly associated with water desorption, and the high-temperature exothermic band is due to the oxidation of organic matter.

The main argument against the reaction mechanism described in Figure 3 might be the high interlayer distance that must be achieved by the new material, which has to be capable of including a bilayer of phenyl groups. With the aim of checking the possibility of a final structure compatible with our hypothesis, we carried out structure modeling starting from the struc-

ture of phlogopite.²⁷ The whole process can be described by the following points.

(1) The symmetry of the phlogopite structure ($C2/m$) was eliminated and the c -axis of the unit cell increased until reproduction of the interlayer distance observed in the diffraction pattern (15.3 Å). The β angle of the monoclinic cell was held constant (100.03°).

(2) The silicate layers were separated to leave empty space enough to host the phenylphosphate groups. Phenylphosphate groups substituted the Mg^{2+} ions of the phlogopite structure so that the P atoms completed a tetrahedral environment bonding to three oxygen atoms of the same layer (two oxygen atoms of the silicate anion and an oxygen atom originally belonging to an OH group). The geometry around the phosphorus atoms was optimized to be tetrahedral.

(3) One of the two silicate layers was slid parallel to the b -axis direction and the phenyl groups were rotated around the P–C bond until the contiguous layers were able to interpenetrate, thus forming a pseudomonolayer.

(27) Rayner, J. H. *Miner. Magn.* **1974**, *39*, 850.

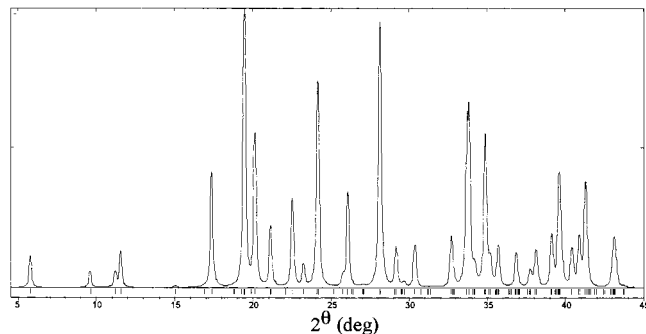


Figure 7. Simulated XRD powder pattern for $K(AlSi_3O_6)(O_3-PC_6H_5)_2$.

Figure 6 indicates that the experimental interlayer distance of the new organic–inorganic hybrid material is consistent with the existence of phenylphosphonic groups in a pseudomonolayer arrangement. The dimensions of the silicate anion make possible the fitting of phenyl groups in this pseudomonolayer. The experimental XRD pattern (Figure 1c) is in agreement with the simulated XRD pattern (Figure 7) generated on the basis of structural data. The differences in reflection intensity are probably due to both the preferred orienta-

tion effects and the true composition of the sample (see Table 1).

Conclusions

The interlayer region of synthetic metal phosphonates can be seen as a well-ordered place in which many reactions of intercalated molecules can take place between these molecules themselves and/or with the organic groups of the layers. The reactivity of layered phosphonates suggests that it might be possible to engineer solids with guest molecules attached according to their shape and chemical properties. Our results show that new types of layered phosphonates can be synthesized using natural minerals as starting materials. The perspectives of application of these new materials are very exciting.²⁸

Acknowledgment. This work was supported by the Ministerio de Ciencia y Tecnología (Spain) and the European Commission, Research Project Nos. 1FD97-1965, BQU2000-0219, and MAT2000-1654.

CM011005D

(28) (a) Vermeulen, L. A.; Thompson, M. E. *Nature* **1992**, *358*, 656.
(b) Dutta, P. *Nature* **1992**, *358*, 621.